Coupled calculation of cavitating nozzle flow, primary Diesel fuel break-up and spray formation with an Eulerian multi-fluid-model

E. v. Berg[1], W. Edelbauer[1], A. Alajbegovic[2], R. Tatschl[1]

1. AVL List GmbH, Hans-List-Platz 1, A-8020 Graz, Austria
2. AVL Powertrain Eng. Inc., 47519 Halyard Drive, Plymouth, MI 48170-2438, USA

A new simulation method for fuel injection is presented. The method is based on the Eulerian multi-fluid approach where separate sets of conservation laws are solved for each phase (or component). Fuel liquid, fuel vapor, spray droplets, and air are treated as interpenetrating phases. Different flow regimes such as cavitating nozzle flow and spray regions are described by using appropriate interfacial exchange terms between the phases. The primary break-up model is based on locally resolved nozzle flow turbulence and is represented as an additional mass exchange term in the spray region. This new approach is applied and validated for a single-hole full scale Diesel injector, and for a large-scale model injector operating water. The results show basic agreement compared to experimental data and yield the correct trends for both spray penetration and spray angle for increasing injection pressure.

Nomenclature

A	area	**M**	Momentum source	**T**	Reynolds stresses	$\sigma_{k,\varepsilon}$	turb. Prandtl num.
C	model parameters	N	Number of phases	t	time	τ	time scale
D	TED source term	N'''	Number density	α_k	volume fraction	τ_k	shear stresses
g	grav. acceleration	P	Pressure	Γ	mass source	Subscripts	
k	turb. kin. energy	P	turb. production	ε	turb. energy dissi.	bub	bubble
K	TKE source term	R	Radius	μ	Viscosity	i	orifice cell index
L	length scale	**V**	Velocity	ρ	Density	k,l	phase indices

1. Introduction

The Diesel jet break-up process during initial stages of droplet formation in injectors is not yet fully understood. In addition to the aerodynamic effects, turbulence and cavitation play an important role in break-up mechanisms. To improve the quality of flow predictions nozzle effects must be introduced directly into the break-up models.
During previous work a procedure was developed at AVL where two separate calculations using the Eulerian two-fluid model inside the injector [1] and the Lagrangian Discrete Droplet Model (DDM) outside the injector in the spray region [2] are performed. With this method flow data obtained from the two-fluid nozzle calculation are transferred into the DDM model as boundary conditions. In addition, a primary break-up model is applied within the DDM. This methodology has certain drawbacks related to its de-coupled nature. One issue is limited temporal resolution of the transient nozzle flow phenomena, caused since only a few nozzle flow data sets are available with linear interpolation between them. In addition the procedure does not take into account feedback between the regions (e.g. re-

circulation) and furthermore does not solve the full set of conservation equations for the bulk liquid phase during the primary break-up process.
A new and promising method is to use the Eulerian multi-fluid approach for both regions simultaneously. The injector and spray regions are represented within a single calculation domain. In this way there is no need for the implementation of artificial boundary conditions. Furthermore this method allows much simpler handling of the calculation.
Primary fuel jet break-up models based on the average values for nozzle flow turbulence have been provided by Huh & Gosman [3] and Bianchi & Pelloni [4]. We extended this approach by using local nozzle flow properties to calculate locally distributed break-up rates and droplet sizes in the orifice cross section [2]. The same model is also used for setting up the primary break-up mass transfer rates in the multi-fluid approach.

2. Model features

2.1. General features of the multi-fluid approach

The multi-fluid model is obtained through the ensemble averaging process (Drew & Passman [5], Lahey & Drew [6]). It treats bubbles, drops, bulk liquid, and vapor as interpenetrating continua. In the spray region the bulk liquid phase disintegrates into various droplet phases. These droplets are characterized by their mean diameter. Furthermore, both vapor and gas are defined as separate phases (or components) within the spray region. The assignment of phases and flow components is given in Table 1.The representation of the different regions within the multi-fluid model is shown in Fig.1.

Table 1. Phases used in coupled calculations

Phase	1	2,...,(n-2)	n-1	n
Contents	gas	droplets	Continuous liquid	vapor

A separate set of conservation equations is solved for each phase. The model equations of the multi-fluid approach are given in Table 2. The inter-phase exchange terms, shown as the summation terms on the equations' right hand side, take into account the effects exerted by one phase onto the other phases and vice versa. They are different for cavitation and spray regions.

2.2. Exchange processes

Mass and momentum interfacial exchange terms are considered, while in the present work we do not consider interfacial heat transfer. Both turbulence kinetic energy (TKE) and turbulence energy dissipation (TED) balance equation are solved for the gas phase separately and for the droplet phases with a homogeneous model, while the corresponding interfacial exchange terms are ignored. The interfacial momentum exchange includes drag forces as well as turbulent dispersion force. Drag formulation is based on a single bubble or droplet drag derived from an ensemble averaging procedure. Turbulent dispersion takes into account turbulence induced diffusion of the dispersed phases in cavitation and spray regions. (see Table 3).

2.2.1. Cavitation induced mass exchange

Mass exchange rate within the nozzle describes vapor generation - evaporation or condensation. Bubble number density N''' is modeled using a heuristic correlation describing decay of number density with increasing volume fraction due to bubble coalescence or vapor film formation. Bubble dynamics is calculated from a linearized Rayleigh-Plesset equation driven by the difference between flow pressure and vapor pressure. The factor c_R in the mass

exchange equation allows treating a delay for onset of re-condensation of the vapor produced. The set of equations used is given in Table 3.

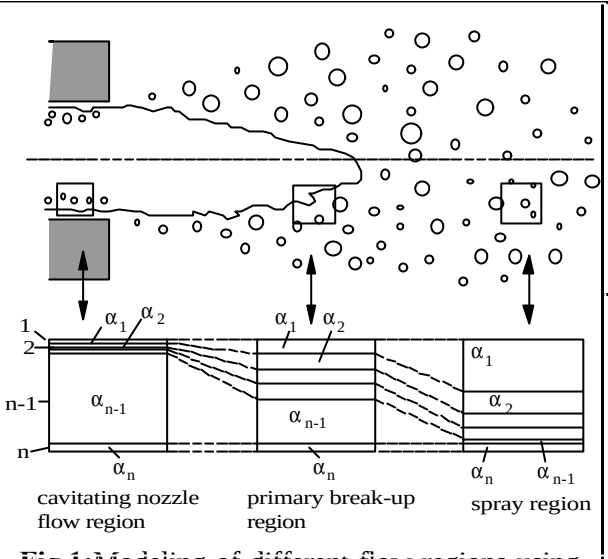

Fig.1: Modeling of different flow regions using volume fraction within multi-fluid approach

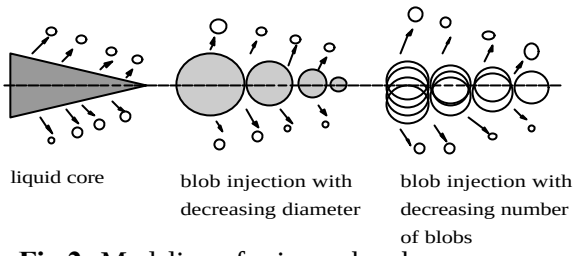

Fig.2: Modeling of primary break-up

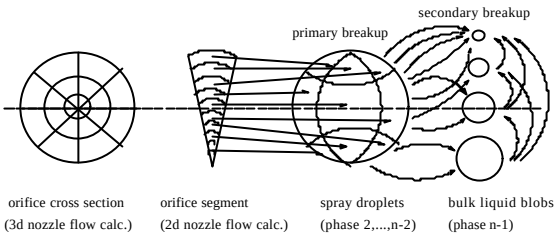

Fig.3: Mapping of orifice to blobs and drops

Table 2. Conservation equations for phases k with k=1,...,n

Mass

$$\frac{\partial \alpha_k \rho_k}{\partial t} + \nabla \cdot \alpha_k \rho_k \mathbf{v}_k = \sum_{l=1, l\neq k}^{n} \Gamma_{kl} \quad , \qquad (1)$$

Compatibility relation

$$\sum_{k=1}^{n} \alpha_k = 1 \qquad (2)$$

Momentum

$$\frac{\partial \alpha_k \rho_k \mathbf{v}_k}{\partial t} + \nabla \cdot \alpha_k \rho_k \mathbf{v}_k \mathbf{v}_k = -\alpha_k \nabla p + \nabla \cdot \alpha_k (\boldsymbol{\tau}_k + \mathbf{T}_k^t) + \alpha_k \rho_k \mathbf{g} + \sum_{l=1, l\neq k}^{n} \mathbf{M}_{kl} + \mathbf{v}_k \sum_{l=1, l\neq k}^{n} \Gamma_{kl} \qquad (3)$$

TKE

$$\frac{\partial \alpha_k \rho_k k_k}{\partial t} + \nabla \cdot \alpha_k \rho_k \mathbf{v}_k k_k = \nabla \cdot \alpha_k \left(\mu_k + \frac{\mu_k^t}{\sigma_k} \right) \nabla k_k + \alpha_k P_k - \alpha_k \rho_k \varepsilon_k + \sum_{l=1, l\neq k}^{n} \mathrm{K}_{kl} + k_k \sum_{l=1, l\neq k}^{n} \Gamma_{kl} \qquad (5)$$

TED

$$\frac{\partial \alpha_k \rho_k e_k}{\partial t} + \nabla \cdot \alpha_k \rho_k \mathbf{v}_k e_k = \nabla \cdot \alpha_k \left(\mu_k + \frac{\mu_k^t}{\sigma_e} \right) \nabla e_k + \sum_{l=1, l\neq k}^{n} \mathrm{D}_{kl} + e_k \sum_{l=1, l\neq k}^{n} \Gamma_{kl} + \alpha_k C_1 P_k \frac{e_k}{k_k} - \alpha_k C_2 \rho_k \frac{e_k^2}{k_k} - \alpha_k C_4 \rho_k e_k \nabla \cdot \mathbf{v}_k \qquad (6)$$

Table 3.	Interphase exchange models for coupled calculation
Momentum exchange for both regions	Drag force: (Indexing applied for spray region!) $\mathrm{M}_{D,1k} = c_D \frac{6\alpha_k \rho_1}{2R_k} \lvert \mathrm{v}_k - \mathrm{v}_1 \rvert (\mathrm{v}_k - \mathrm{v}_1)$ (7) for k=2,..,n-1 Turbulent dispersion force: $M_{T,1k} = c_{T,1k} \rho_1 k_1 \nabla \alpha_k$ (8)
Cavitation Mass exchange	Mass transfer rate $\Gamma_{n-1,n} = \rho_n \frac{N'''}{c_R} 4\pi R_{bub}^2 \frac{\partial R_{bub}}{\partial t}$ (9) Bubble radius $R_{bub} = \sqrt[3]{\frac{3\alpha_n}{4\pi N'''}}$ (10) Bubble radius rate of change $\frac{dR_{bub}}{dt} = sign(\Delta p) \sqrt{\frac{2\Delta p}{3\rho_{n-1}}}$ (11)
Spray mass exchange	Primary break-up (12) $\Gamma_{n-1,k} = \frac{3\alpha_{n-1}\rho_{n-1}}{R_{n-1}A_{noz}} \sum_i \frac{\mathrm{A_i L_i}}{t_i} = -\Gamma_{k,n-1}$ with k = 2,..., n - 2 and i sampling contributions to class k Secondary break-up $\Gamma_{k,l} = \frac{3\alpha_k}{R_k} \rho_k \frac{R_k - R_{stable}}{\tau_k} = -\Gamma_{l,k}$ with $1 < l <$ k and k = 2,....,n-3 (13)

2.2.2. Interfacial mass exchange within the spray region

Mass transfer within the spray region takes into account primary break-up of the bulk liquid phase according to the model of Bianchi & Pelloni [4], applied within each cell. The model uses turbulent length scale to determine the atomization length scale and also the droplet size. Break-up time scale is calculated from a weighted mean of turbulent and aerodynamic time scales. The aerodynamic time scale is calculated assuming break-up due to Kelvin-Helmholtz instability at the liquid surface. From atomization length scales L_i and time scales τ_i finally the mass exchange rate due to primary break-up is calculated according to Equation (12) in Table 3. The radial droplet start velocity is estimated as the ratio between the characteristic atomization length scale and the break-up time scale. This value is used to determine the direction of the momentum transfer vector from primary break-up.
The droplets produced from the primary break-up process are subject to further secondary break-up processes. These are modeled using the standard WAVE break-up model, which has been translated into the Eulerian frame [7]. This is applied to all of the droplet phases in each cell of the spray region. If the predicted size of break-up products is less than the parent drop diameter, there is mass transfer according to the break-up rate into the corresponding droplet size class, where the product droplet size fits in. The break-up model equations are provided in more detail in [2,7].

2.3. Coupling between nozzle and spray regions

Since the basic transport equations are the same in both regions the transition between flow regimes can be realized by switching from cavitation exchange terms to spray exchange terms at the nozzle orifice. In the simplest case this could be done immediately in the orifice cross section. However, under realistic conditions the transition from nozzle flow to spray is established by a continuous primary break-up process, which causes disintegration of the continuous liquid phase over a certain distance. Besides yielding a more physical model this also enhances numerical stability due to smoothing of the source term gradients. Further, all information from nozzle flow is easily available in full detail to calculate the break-up rates according to the model sketched above.
In principle, the multi-fluid approach is capable to treat arbitrary shapes of the interfacial area entering the exchange terms. The present application primarily deals with drops or bubbles. As a first step approach, a spherical shape is assumed. A predefined droplet diameter is assigned to each of the phases. The coherent liquid structure of the disintegrating bulk liquid phase has been idealized as a series of large blobs with size of the nozzle hole diameter. According to the classical blob injection method used within the Lagrangian DDM, the blobs decrease in diameter and release the primary spray droplets. This picture is further simplified by assuming constant diameter of the parent drops. Thus, mass loss appears as a reduction of number of drops with fixed diameter (see Fig. 2). Since this underestimates the exchange area, future model improvements with this respect are necessary.
Fig. 3 shows how the nozzle flow properties are mapped to the surface of the blobs, which represent the disintegrating bulk liquid phase inside the spray domain. According to Fig. 3 the primary break-up model is applied for each blob surface element, which are again linked to the surface elements in the orifice. Single mass flow contributions are sorted according to the product droplet diameters into the desired number of (n-3) droplet size classes. In the further course of the calculation these droplet phases may additionally exchange mass according to secondary break-up process.

3. Results

The coupled calculation of injector flow and spray formation has been compared with experimental data from Diesel injection via a straight single hole nozzle with 0.2 mm diameter operated under realistic conditions of 30 to 120 MPa injection pressure and 2 MPa chamber pressure at ambient temperature. For this nozzle a 10-degree sector has been calculated using radial symmetry. The corresponding experiments have been performed at Robert Bosch GmbH [8] and DaimlerChrysler Research [9] in the frame of the I-LEVEL project funded by the CEC.
Further comparisons have been performed with a large-scale model injector of 5-mm nozzle hole diameter operated with water at a pressure difference between 0.2 and 0.1 MPa. For the model injector one half of the geometry has been used to catch the strong 3D effects occurring in this configuration with single injection hole mounted perpendicular to the feed tube axis. These experiments have been performed at Chalmers University [10]. They provide good optical insight to cavitation as well as spray cone formation.
The unstructured hybrid calculation grids are shown in Figures 4 and 5. Different flow scales in the nozzle and spray regions have been taken into account by a fine mesh in the nozzle and a coarser mesh in the spray region. The latter has been compressed towards the nozzle and additionally refined close to the nozzle. Different mesh regions have been linked with arbitrary interfaces. For the Diesel injector the total cell number is about 3850, covering a total length of 0.12 m. For the model injector about 15000 cells have been used with refinements inside and close to the injection hole. The modeled part of the feed tube is about 6 cm long; the spray region has similar extension length.

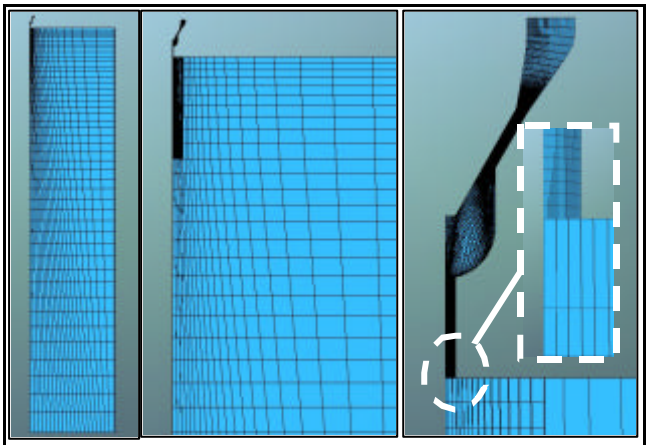

Fig.4: Computational grid of the Diesel injector

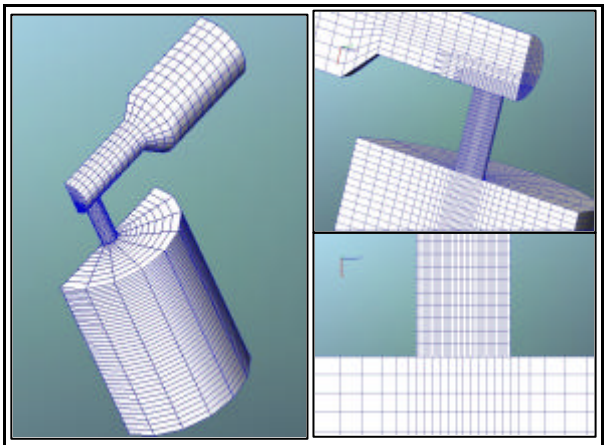

Fig.5: Computational grid Chalmers case

3.1. Basic features

Some basic features of the results gained from the coupled calculations are shown in Fig. 6 and Fig. 7 for the Diesel injection case at an injection pressure of 30 MPa. This case has been calculated with four droplet phases, bulk liquid phase and two gaseous phases for fuel vapor and air. Figure 6 shows the volume fractions of the droplet phases 2 to 5 and the bulk liquid phase. It can be clearly seen how the bulk liquid phase volume fraction decreases due to primary break-up. This causes mass transfer to all of the droplet phases. The largest amount enters phase 5. All of the droplet phases are subject to secondary break-up according to the WAVE model. This causes an additional redistribution of mass, which finally yields a mass distribution with concentration of the mass in the smallest droplet size class of phase 2. Furthermore, close to the nozzle there is also an accumulation of mass in phase 5 coming form the primary break-up, which is again reduced far downstream by the secondary break-

up. Figure 7 shows the velocity distributions of all phases. It can be seen that near the nozzle gas is entrained and accelerated by the drops, while further downstream there is again velocity decay according to expansion and further mixing. In contrast to this, the vapor phase emanating from the nozzle has higher velocities. The bulk liquid phase, which is modeled by large blobs, as well as the droplet phases show decreasing velocity along the centerline and also in radial direction according to the drag forces acting between the phases. This effect is most pronounced for the phase with smallest drop size, as expected from the larger exchange area.

3.2. Comparison with experimental data for 2D Diesel injection case

The described model has been already applied to a series of Diesel fuel injection experiments with rail pressure increasing from 30 to 120 MPa. Seven phases have been used distributed according to Table 1. Model parameters have been adjusted to match with the 50 MPa case. The cavitation settings have been adjusted to give approximately the same mean vapor film thickness as in the experiment [8]. Similarly, spray parameters have been set to yield spray angle and penetration close to the reference case. All other calculations have been performed with the same parameter sets. Fig. 8a) shows a comparison between the calculated spray contours and the shapes measured in the experiments. For comparison, iso-line plots for the total volume fraction of the liquid phases have been used. A problem with the Eulerian spray

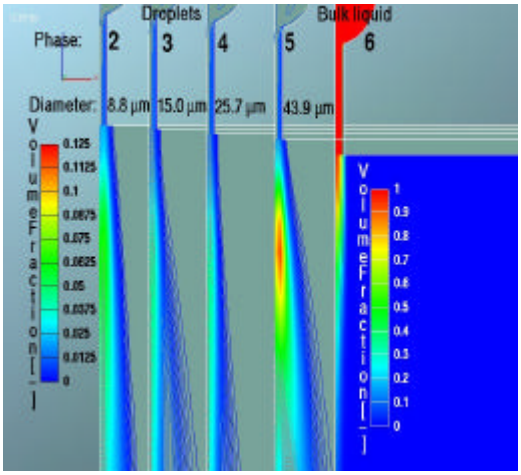

Fig. 6: Volume fraction of coupled calc.

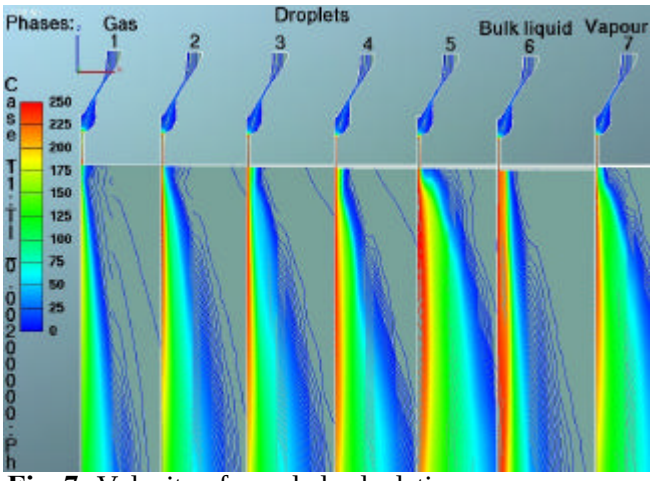

Fig. 7: Velocity of coupled calculation

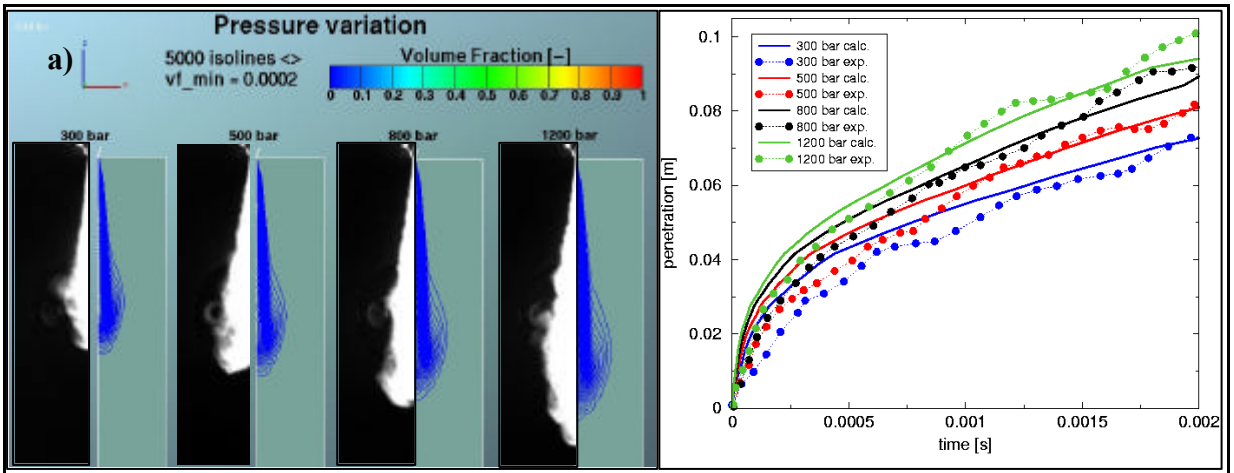

Fig. 8: Comparison of Diesel test case with experimental data for variation of injection pressure: a) spray contours, b) spray penetration

model is that the spray boundary is not as easy to detect as in the Lagrangian DDM. Thus, a limiting threshold value for the total volume fraction has been determined from the reference case. As can be seen in Fig. 8a) the results show basic agreement with the overall shape of the spray and also yield the correct penetration which increases with increasing injection pressure. Fig. 8b) shows the spray tip penetration curves, further confirming good agreement with the experimental data.

3.3 Comparison with experimental data for 3D model nozzle

The Chalmers University model injector was simulated using a total of five (5) phases. Injection pressure varied between 0.2 and 0.3 MPa in the calculations. The results have been compared with the experimental data for cavitation structure as well as for the spray contour. A remarkable feature of this experiment is the strengthening asymmetry of the spray cone with increasing injection pressure. This is due to flow deflection caused by the asymmetric cavitation region [2]. This effect is additionally enhanced by the primary break-up process, which is also asymmetric due to inhomogeneous distribution of turbulence parameters in the nozzle orifice. Figure 9 shows a comparison between total liquid volume fraction and spray contours from the experiments for different injection pressures. Despite the fact that the spray angle seems to be somewhat under-estimated, there is considerably good agreement with the overall shape of the spray. The trend of increasing asymmetry with increasing pressure is clearly visible. Figures 9b) and 9c) show a detailed comparison between the experimental spray contours and the simulation using the Eulerian model and the Lagrangian DDM. It can be seen that in the nozzle proximity the flow structure is resolved in more detail by the coupled approach as well as the shape of the spray contour.

4. Conclusions

A new methodology for coupled calculation of cavitating nozzle flow, primary fuel jet break-up and spray formation and propagation has been developed. This method is based on the

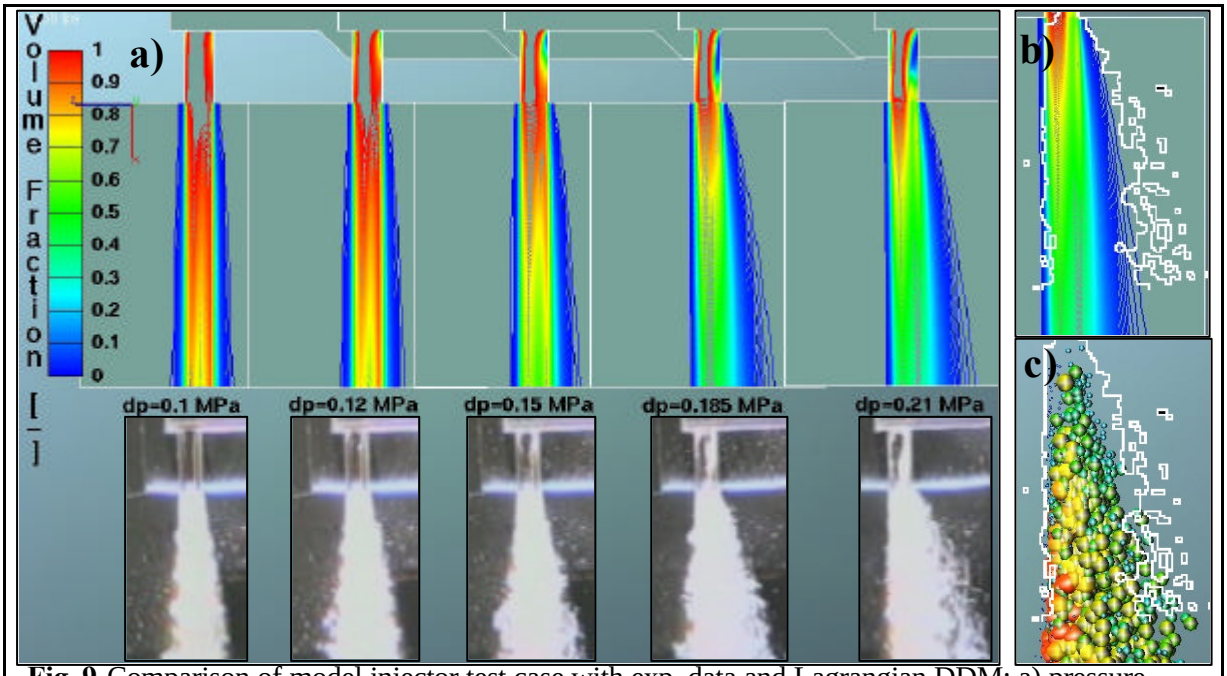

Fig. 9 Comparison of model injector test case with exp. data and Lagrangian DDM: a) pressure variation, b) case 5 with Eulerian model, c) case 5 with Lagrangian DDM

Eulerian multi-fluid approach available in the AVL FIRE CFD code. The physics of different flow regimes is introduced via appropriate interfacial exchange terms between the phases that differ in the nozzle and spray regions. In the coupled approach interfacial mass exchange for cavitation, primary and secondary droplet break-up processes is included. Momentum exchange terms include drag force and turbulent dispersion force. The model has been tested for both Diesel injector flow under realistic conditions and for a large-scale model injector. The results are promising and predict the overall features of the experimental data over a wide range of injection conditions. The applied models give correct trends for spray penetration and asymmetry of the spray angle. Especially the latter has also been detected in recent experimental analysis of multi-hole Diesel injectors [11].
The major advantage of the coupled approach is the natural link between the cavitating nozzle flow and the downstream spray break-up behavior. This allows detailed and robust modeling of the overall injection process. The presented model constitutes a promising platform for future development.

5. Acknowledgements

This study is partly based on funding by the European Commission in the framework of the Growth Program (Project Number: GRD1-1999-10034). The experimental nozzle flow data have been prepared by Dr. Jochen Walther at Robert Bosch GmbH; the spray data were measured by Dr. Gerhard König at DaimlerChrysler Research Department. David Higbie at AVLNA greatly improved the style of the paper. The authors would like to thank very kindly for this helpful support.

6. References

[1] A. Alajbegovic, G. Meister, D. Greif, B. Basara: Three phase cavitating flows in high-pressure swirl injectors. Experimental Thermal and Fluid Science, 2002, 26(2002) 677-681

[2] E. v. Berg, W. Edelbauer, R. Tatschl, A. Alajbegovic, M. Volmajer, B. Kegl and L. Ganippa: Validation of a CFD model for coupled simulation of nozzle flow, primary fuel jet break-up and spray formation. Proc. ICES03, ASME, Salzburg, Austria, May 11-14, 2003

[3] K.Y. Huh and A.D. Gosman: Phenomenological Model of Diesel Spray Atomisation. Proc. Int. Conf. on Multiphase Flows, Sept. 24-27, Tsukuba, Japan, 1991

[4] G. Bianchi, P. Pelloni: Modelling the Diesel Fuel Spray Break-up by Using a Hybrid Model. SAE 1999-01-0226

[5] Drew, D.A., Passman, S.L., Theory of Multicomponent Fluids, Springer, New York, 1998.

[6] Lahey, R.T., Jr., Drew, D.A., An Analysis of Two-Phase Flow and Heat Transfer Using a Multidimensional, Multi-Field, Two-Fluid Computational Fluid Dynamics (CFD) Model, Japan/US Seminar on Two-Phase Flow Dynamics, Santa Barbara, California (2000).

[7] E. v. Berg, A. Alajbegovic, R. Tatschl, C. Krüger and U. Michels: Multiphase Modeling of Diesel Sprays with the Eulerian/Eulerian Approach. Proc. of 17th ILASS-Europe Conf., September 2-6, 2001, Zurich

[8] J. Walther: Quantitative Untersuchungen der Innenströmungen in kavitierenden Diesel-einspritzdüsen, Dissertation, TU Darmstadt, 2002

[9] Private communication: Dr. G. König, DaimlerChrysler Research, Stuttgart, Germany

[10] L.C. Ganippa et al.: The Structure of Cavitation and its Effect on the Spray Pattern in a Single-Hole Diesel Nozzle. SAE-Paper 2001- 01-2008

[11] G. König, M. Blessing, C. Krüger, U. Michels and V. Schwarz: Analysis of Flow and Cavitation Phenomena in Diesel Injection Nozzles and its Effects on Spray and Mixture Formation. 5th Int. Symposium on Combustion Diagnostics, June 6-7, 2002, Baden-Baden, Germany